GANT-61 Induces Autophagy and Apoptosis in Glioblastoma Cells despite their heterogeneity

Gabriela Basile Carballo[1,2,3] · Jessica Honorato Ribeiro[1,2,4] · Giselle Pinto de Faria Lopes[2,5] ·
Valéria Pereira Ferrer[2,6] · Romulo Sperduto Dezonne[7] · Cláudia Maria Pereira[7] ·
Tania Cristina Leite de Sampaio e Spohr[1,2]

Abstract

Glioblastoma (GBM) is the most common adult primary tumor of the CNS characterized by rapid growth and diffuse inva-
siveness into the brain parenchyma. The GBM resistance to chemotherapeutic drugs may be due to the presence of cancer
stem cells (CSCs). The CSCs activate the same molecular pathways as healthy stem cells such as WNT, Sonic hedgehog
(SHH), and Notch. Mutations or deregulations of those pathways play a key role in the proliferation and differentiation of
their surrounding environment, leading to tumorigenesis. Here we investigated the effect of SHH signaling pathway inhibi-
tion in human GBM cells by using GANT-61, considering stem cell phenotype, cell proliferation, and cell death. Our results
demonstrated that GANT-61 induces apoptosis and autophagy in GBM cells, by increasing the expression of LC3 II and
cleaved caspase 3 and 9. Moreover, we observed that SHH signaling plays a crucial role in CSC phenotype maintenance,
being also involved in the epithelial-mesenchymal transition (EMT) phenotype. We also noted that SHH pathway modulation
can regulate cell proliferation as revealed through the analysis of Ki-67 and c-MYC expressions. We concluded that SHH
signaling pathway inhibition may be a promising therapeutic approach to treat patients suffering from GBM refractory to
traditional treatments.

✉ Tania Cristina Leite de Sampaio e Spohr
  tcspohr@gmail.com

1 Instituto Estadual Do Cérebro Paulo Niemeyer, Rua do
   Rezende 156, Rio de Janeiro, RJ 20231-092, Brazil

2 Programa de Pós-Graduação em Anatomia Patológica,
   Hospital Universitário Clementino Fraga Filho, Universidade
   Federal Do Rio de Janeiro, Rio de Janeiro, Brazil

3 Orofacial Development and Regeneration, Institute of Oral
   Biology, Centre for Dental Medicine, University of Zurich,
   Zurich, Switzerland

4 Radiobiology Unit, Belgian Nuclear Research Centre,
   SCK·CEN, Mol, Belgium

5 Departamento de Biotecnologia Marinha, Instituto
   de Estudos do Mar Almirante Paulo Moreira
   (IEAPM)/Coordenação de Pesquisa, Instituto Nacional de
   Câncer (INCA), Rio de Janeiro, RJ, Brazil

6 Department of Cellular and Molecular Biology,
   Institute of Biology, Fluminense Federal University,
   Niteroi, Rio de Janeiro, Brazil

7 Programa de Pós-Graduação em Biomedicina Translacional,
   Universidade Do Grande Rio, Duque de Caxias, Brazil

Abbreviations

AO	Acridine orange
ATTC	American Tissue Culture Collection
AVOs	Acidic vacuolar organelles
BSA	Bovine serum albumin
CNS	Central nervous system
CSCs	Cancer stem cells
DAPI	4–6-Diamino-2-phenylindole
DMEM/F-12	Dulbecco's medium supplemented with F-12
DMSO	Dimethyl-sulfoxide
EMT	Epithelial-mesenchymal transition
FBS	Fetal bovine serum
GBM	Glioblastoma
GANT-61	GLI-ANTagonist 61
IECPN	Instituto Estadual do Cérebro Paulo Niemeyer
IF	Immunofluorescence
MTT	3-(4, 5-Dimethylthiazol-2-yl)-2,5-diphenyl tetrazolium bromide
PBS	Phosphate-buffered saline

PFA	Paraformaldehyde
PI	Propidium iodide
PTCH	Patched
PVDF	Polyvinylidene difluoride
qRT-PCR	Quantitative PCR
rh-SHH	Recombinant Sonic Hedgehog/ SHH(C24II)
SHH	Sonic hedgehog
SMO	Smoothened
SuFu	Suppressor of Fused
TBS-T	Tris-buffered saline with 0.1% Tween-20
TGF-β	Transforming growth factor-beta
TMZ	Temozolomide
WB	Western Blot

Introduction

Cancer mortality and incidence worldwide is rapidly growing. In 2018, there was an estimate of 18.1 million new cancer cases with 9.6 million cancer deaths, being 296,851 new brain cancers with 241,037 deaths (Bray et al. 2018). Glioblastoma (GBM) is the most common adult and malignant primary tumor of the central nervous system (CNS), and it is characterized by rapid growth and diffuse invasiveness into the adjacent brain parenchyma rendering surgical resection inefficient (Nakada et al. 2011; Ostrom et al. 2018). Therefore, GBM is considered to be one of the most difficult human malignancies to manage, also due to frequent dysfunctions of tumor suppressors and oncogenes and deregulation of several genetic and molecular pathways that allows recurrence of this tumor (Bonavia et al. 2011; Carballo et al. 2018b; Geraldo et al. 2019). It is believed that most of the cancers, including GBM, are resistant to chemotherapeutic drugs due to the presence of a cancer stem cell (CSC) subpopulation, which ultimately leads in tumor relapse and consequently decreases patient survival (Dean et al. 2005; Ponnusamy and Batra 2008). CSCs usually undergo several mutations that promote tumorigenesis. These cells require the assistance of a corrupted microenvironment giving support for their growth (Hanahan and Coussens 2012). The major features attributed to these mutated stem cells affect their abilities to self-renew, chemoresistance, and epithelial-mesenchymal transition (EMT) phenotype. They typically exploit the same molecular pathways that regulate healthy stem cells such as WNT, Sonic hedgehog (SHH), Notch, as wells as others molecules activated during embryogenesis and organogenesis (Roth et al. 2000; Golestaneh and Mishra 2005; Geraldo et al. 2019).

The SHH pathway regulates the embryonic development of both invertebrates and vertebrates (Kimura et al. 2005). In adults, mutations and/or deregulations of this pathway play a crucial role in both proliferation and differentiation

of their surrounding environment, leading to tumorigenesis (Dahmane et al. 1997; Bailey et al. 2007; Kurebayashi et al. 2017). Besides, high GLI1 expression in GBM is considered an inherently negative prognostic factor associated with CSC maintenance, being GLI1 is a key regulator of target-stemness genes in response to SHH activation (Villavicencio et al. 2000; Rossi et al. 2011). The SHH pathway activation occurs in two major ways, canonical and non-canonical. The canonical signaling occurs through the co-receptor Smoothened (SMO), while the non-canonical is independent of SMO (Carballo et al. 2018a). Briefly, upon ligand binding to Patched (PTCH), SMO is released, resulting in SHH pathway activation and transcription of target genes, including GLI1, GLI2, PTCH1, and stemness genes such as Nanog, OCT-4, and SOX-2. In the absence of ligand, the SHH receptor PTCH inhibits the co-receptor SMO (Taipale et al. 2000; Clement et al. 2007; Carballo et al. 2018b).

It was previously demonstrated that blocking SHH signaling with cyclopamine, which specifically acts on SMO (canonical), or using GLI-ANTagonist 61 (GANT-61) (canonical and non-canonical) that acts on GLI1/2, inhibits tumor cell proliferation and suppresses tumor formation (Lauth et al. 2007; Von Hoff et al. 2009). Besides, studies have shown that GANT-61 affects several hallmarks of cancer such as proliferation, cell viability, apoptosis, autophagy, EMT, and CSC markers in different types of cancers including neuroblastoma and rhabdomyosarcoma (Benvenuto et al. 2016; Gonnissen et al. 2016). Moreover, GANT-61 decreased in a time and dose-dependent manner GLI1 and GLI2 mRNA levels in breast cancer cell lines (Koike et al. 2017). Since SHH is highly expressed in GBM and it could be modulated by GANT-61, we investigated the effect of SHH signaling pathway inhibition on human GBM cells through GANT-61 analyzing their stemness state, cell proliferation, and cell death mechanisms. Here, we demonstrate that GANT-61 induced apoptosis and autophagy in GBM cells, by increasing the expression of LC3 II and cleaved caspases 3 and 9.

Materials and Methods

Reagents

All culture reagents as well as the secondary antibodies, conjugated to Alexa Fluor 488, 546 and HRP, Prolong Gold Antifade reagent, BCA™ Protein Assay kit, Super Signal™ West Pico or West Femto Chemiluminescent Substrate, Trizol, oligodT (12–18) primer, High-Capacity cDNA Reverse Transcription Kit and Power Sybr Green Master Mix, MicroRNA Reverse Transcription kit and hsa-miR-17-5p cat nº 02308, hsa-miR-326 cat nº 000542, and RNU48 cat nº 001006 primers were obtained from Thermo

Fisher Scientific (Waltham, Massachusetts, USA). Dulbecco's medium supplemented with F-12 (DMEM/F-12) and fetal bovine serum (FBS) was purchased from Gibco (Massachusetts, USA). Recombinant Sonic Hedgehog/SHH (C24II) (rh-SHH) was purchased from Peprotech (São Paulo, BR). Paraformaldehyde (PFA) was purchased from Isofar (Rio de Janeiro, Brazil). The 4–6-diamino-2-phenylindole (DAPI), 3-(4, 5-dimethylthiazol-2-yl)-2,5-diphenyl tetrazolium bromide (MTT), dimethyl-sulfoxide (DMSO), propidium iodide (PI), citrate buffer, acridine orange (AO), bovine serum albumin (BSA), and anti α-tubulin were purchased from Sigma-Aldrich Corp. (St. Louis, MO, USA). Triton X-100 was purchased from LGC Biotecnologia (São Paulo, Brazil); polyclonal antibody anti-GLI1 was purchased from EMD Millipore Corporation, Temecula, CA, USA, cat nº ABC217. Monoclonal mouse anti-human Ki-67 antigen cat nº M740 and monoclonal mouse anti-Vimentin Clone V9 cat nº M0725 were purchased from Dako, Glostrup, Denmark. Polyclonal anti-NANOG (D73G4) XP rabbit mAb cat. nº 4903, polyclonal anti-OCT-4A (C30A3) rabbit mAb cat. nº 2840, anti-caspase 3 rabbit mAb cat nº9662, caspase-9 (C9) mouse mAb monoclonal cat nº 9508, c-MYC (D84C12) Rabbit mAb cat nº 5605, polyclonal anti-SOX-2 (D6D9) XP rabbit mAb cat. nº 3579, and Phospho p70 S6 Kinase (Thr389) antibody cat nº 9205 were purchased from Cell Signaling Technology, Danvers, MA, USA. Anti-Patched/PTCH1 antibody cat nº ab53715, anti-GAPDH [6C5] antibody cat nº ab8245, and anti-Sonic Hedgehog antibody [EP1190Y] cat nº ab53281 were purchased from Abcam, Cambridge, United Kingdom. Hybond-P polyvinylidene difluoride (PVDF) transfer membrane was obtained from Bio-Rad Laboratories (Berkeley, CA, USA). GANT-61 was obtained from Tocris Bioscience, cat nº 3139, Bristol, UK. Anti-LC3B/MAP1LC3B Antibody was obtained from Novus Biologicals, Littleton, CO, USA, cat nº NB600-1384.

Cell Culture

The human GBM cell line T98G was obtained from the American Tissue Culture Collection (ATCC) (USA), and the cell line GBM11 and the human astrocytes were established and characterized in our laboratory as previously described for other cell lines (Faria et al. 2006). Briefly, GBM11 cells were obtained by surgical biopsy from a 57-year-old male patient bearing a recurrent primary GBM previously treated with temozolomide (TMZ) concomitantly with radiotherapy, who had given written consent to the study. The human astrocytes were isolated from an epileptic patient submitted to surgery and came from the temporal lobe. All procedures were in agreement with the Brazilian Ministry of Health Ethics Committee (CONEP no. 738/2001 and IECPN CAAE nº 90670018.4.0000.8110), as previously described (Balça-Silva et al. 2017). The tumor cells were termed GBM11.

The cells were cultured in DMEM-F-12 supplemented with 3.5 mg/mL glucose, 0.1 mg/mL penicillin, 0.14 mg/mL streptomycin, and 10% FBS. The cultured cells were maintained at 37 °C in an atmosphere of 95% air and 5% CO_2. In all conditions, we used a concentration of 20 μM of GANT-61 and the concentration of 2 ng/mL of rh-SHH, N-Terminus in DMEM/F-12 with 5% FBS. The cells were treated during 48 h or 8 days with 2 ng/mL rh-SHH diluted in MWS 5% or with 20 μM of GANT-61 diluted in MWS 5%. The control cells were cultivated only with MWS 5% and the same amount of DMSO used to dilute GANT-61. To cells treated for 8 days, we changed the medium every 4 days. The written informed consent for the isolation of cells to establish a new cell line for future research was obtained from the patient himself before the surgery.

Immunofluorescence (IF) Staining

This was performed as previously described (Spohr et al. 2011). Briefly, GBM cells were fixed with 4% PFA for 20 min and permeabilized with 0.2% Triton X-100 for 30 min at 24 °C, if the staining was to intracellular protein or fixed only for 5 min without cell permeabilization with Triton-X-100 if the staining was to extracellular protein. After, the cells were blocked with 5% BSA in phosphate-buffered saline (PBS) (blocking solution) for 1 h and incubated overnight at 4 °C with specified primary antibodies diluted in blocking solution. Primary antibodies were polyclonal antibody anti-GLI (1:400); monoclonal mouse anti-human Ki-67 antigen (1:200); anti-NANOG (D73G4) XP rabbit mAb (1:400); anti-OCT-4A (C30A3) rabbit mAb (1:400); anti-Patched/PTCH1 antibody (1:50); anti-Sonic Hedgehog antibody [EP1190Y] (1:200); anti-SOX-2 (D6D9) XP rabbit mAb (1:400); monoclonal mouse anti-Vimentin Clone V9 (1:100). After primary antibody incubation, cells were extensively washed with $1 \times$ PBS and incubated with secondary antibodies for 1 h, at 24 °C. The secondary antibodies were goat anti-rabbit IgG conjugated with Alexa fluor 488 (1:750) and goat anti-mouse IgG conjugated with Alexa fluor 546 (1:1000). The nuclei were stained with DAPI. Negative controls were performed by omitting the primary antibody during staining. In all cases, no reactivity was observed when the primary antibody was absent. Cell preparations were mounted directly on the Prolong Gold Antifade reagent and visualized by using a DMi8 advanced fluorescence microscope (Leica Microsystems, Wetzlar, Germany). The fluorescence intensity of individual cells was measured and analyzed using ImageJ software (NIH).

Quantitative PCR (qRT-PCR)

RNA isolation and reverse transcription were performed as described previously (Matias et al. 2018). Briefly, total

RNA was purified using the Purelink RNA Mini kit (Thermo Fisher Scientific) following the manufacturer's instructions. One microgram of the total RNA, oligodT (12–18) primer (Thermo Fisher Scientific), and High-Capacity cDNA Reverse Transcription Kit (Applied Biosystems) were used to perform the cDNA synthesis following the manufacturer guide. For qPCR, we used the SSO Advanced Universal Sybr Green Supermix (Bio-Rad), and 46 ng of cDNA per well of the T98G or GBM11 samples. qRT-PCR reactions were carried out in triplicate using the CFX96 Real-Time PCR system (Bio-Rad). Cycling conditions were 95 °C/10 min followed by 40 cycles at 95 °C/15 s and 60 °C/30 min. Relative quantification of targeted mRNA levels was performed using the Pfaffl method (Pfaffl 2001), GAPDH as an endogenous gene, and samples untreated as the control. The primers employed in this study are *GLI1* Forward (5′-TTCCTACCAGAGTCCCAAGT-3′); *GLI1* Reverse (5′-CCC TATGTGAAGCCCTATTT); *PTCH1* Forward (5′-TGACCT AGTCAGGCTGGAAG-3′); *PTCH1* Reverse (5′-GAAGGA GATTATCCCCCTGA-3′); *SMO* Forward (5′-TCGCTACCC TGCTGTTATTC-3′); *SMO* Reverse (5′-GACGCAGGACAG AGTCTCAT-3′); *GAPDH* Forward (5′-GAGTCAACGGAT TTGGTCGT-3′); *GAPDH* Reverse (5′-TTGATTTTGGAG GGATCTCG-3′).

Real-Time PCR for miRNAs

Thirty nanograms of total RNA were reverse-transcribed in miR-17-5p, miR-326-5p, and RNU48cDNAs using the MicroRNA Reverse Transcription kit and miRNA-specific primers (hsa-miR-17-5p, hsa-miR-326, and RNU48). The cDNA synthesis conditions were 16 °C for 30 min, 42 °C for 30 min, and 85 °C for 5 min. Real-time PCR was performed using a standard protocol and carried out in a QuantStudio 7 Detection System (Thermo Fisher Scientific, Waltham). The samples were run in triplicate, in a total volume of 20 μL, with its proper negative controls. The conditions for real-time PCR amplification were 50 °C for 2 min, 95 °C for 10 min, followed by 40 cycles of 95 °C for 15 s and 60 °C for 1 min. The relative expression of each miRNA was normalized against RNU48. Analysis of miRNA expression followed the 2-ΔΔCq method (Livak and Schmittgen 2001). Calculation of the formula ΔΔCq involves then subtracting the value of ΔCq for each experimental sample from the value of ΔCq for the calibrator samples. To consider a miRNA over- or under-expressed, an arbitrary fold-change value of ± 2 was adopted.

Protein Quantification and Western Blot (WB) Analysis

GBM cells were cultured in 6-well plates and incubated for 8 days in the presence of either 2 ng/mL rh-SHH or GANT-61 20 μM or control condition. Then, the cells were washed with $1 \times$ PBS, scraped off using a rubber policeman, and a lysis buffer was added (Tris base 10 mM, saccharose 0.25 M, EDTA 1 mM, in the presence of protease inhibitors). The lysates were sonicated and then centrifuged at 4 °C, $10,000 \times g$ for 10 min. Protein concentration on cell extracts was measured in triplicate by the Pierce™ BCA Protein Assay kit. Twenty micrograms of protein per lane were electrophoretically separated in 8 or 10 or 12% sodium dodecyl sulfate–polyacrylamide homemade gels. After separation, the proteins were electrically transferred to the PVDF transfer membrane for 4 h using the wet method or for 17 min using the Trans-Blot Turbo™ Transfer-System (Bio-Rad Laboratories Inc, Hercules, CA, USA). The membranes were then blocked with 5% non-fat milk or with BSA 5% in Tris-buffered saline with 0.1% Tween-20 (TBS-T) depending on the primary antibody used, for 1 h. Then the membranes were incubated with specific primary antibodies overnight at 4 °C, washed with 0,1% TBS-T, and incubated with peroxidase-conjugated antibodies. The primary antibodies used were anti-OCT-4A (C30A3) rabbit mAb (1:1000); anti-Patched/PTCH1 antibody (1:500); anti-Sonic Hedgehog antibody [EP1190Y] (1:1000); anti-SOX-2 (D6D9) XP rabbit mAb (1:1000); monoclonal mouse anti-Vimentin Clone V9 (1:500); anti-LC3B/MAP1LC3B Antibody (1:1000); anti-GAPDH antibody [6C5] (1:2500); anti Phospho p70 S6 Kinase (Thr389) antibody (1:1000), c-MYC (1:1000), caspase-3 antibody (1:1000) and caspase-9 (C9) mouse mAb antibody (1:1000). The secondary antibodies used were secondary peroxidase-conjugated antibodies were goat anti-rabbit IgG (1:1000) and goat anti-mouse IgG (1:1000). The staining was detected using ECL and chemiluminescence detection, with the ChemiDoc MP imaging system (Laboratories Inc, Hercules, Benicia, CA, USA). The densitometric analysis was obtained using Bio-Lab Software (Bio-Rad, Berkeley, USA). Values represent the ratio between the GAPDH or α-tubulin as the loading control and protein levels for each sample.

MTT Assay

Cell viability was assessed by MTT assay. Briefly, 10,000 of GBM11 cells or 8000 of T98G cells (for 48 h) or 3000 of GBM11 or 1000 of T98G cells (8 days) per well were seeded into 96-well micro-culture plates at 37 °C with 5% CO_2 together with rh-SHH 2 ng/mL, GANT-61 20 μM, or control condition, for the experiments that take 48 h or 8 days, respectively. After the treatment, the cells were incubated with MTT at the final concentration of 0.5 mg/mL for 2 h before the completion of exposure time at 37 °C. The formation of MTT to formazan crystals by viable cells was assessed using 50 μL/well DMSO at room temperature for 20 min. Optical density was measured at 570 nm

using Multimode Plate Reader Victor™ X3 (Perkin Elmer, Waltham, MA, USA). The reduction in viability of cells in each well was expressed as the percentage of the control cells.

Cell Cycle and DNA Fragmentation Analysis

T98G (29,000 cells/well) and GBM11 cells (82,000 cells/well) were seeded in 6-well plates, followed by rh-SHH and/or GANT-61 treatment. After 48 h or 8 days of incubation, cells were incubated with a citrate buffer solution (pH 6.0) containing PI (50 μg/mL), 0.3% Triton X-100, and RNAse (100 μg/mL) for 30 min in the dark at room temperature. The DNA content was accessed by flow cytometry at 575/25 nm (FL2 channel) (FACS Calibur flow cytometer, Becton & Dickinson, USA) and 10,000 events at least were acquired. In three independent experiments at least, DNA content was analyzed using Summit v4.3 software (Beckman-Coulter, CA, USA) as the percentage of a cell population in each cell cycle phase (G_0/G_1, S, G_2/M) and fluorescence in sub-G_0/G_1 was considered DNA fragmentation.

Acidic Vacuolar Organelles (AVOs) by Acridine Orange (AO)

The development of AVOs is a typical feature of autophagy because only mature/late autophagosomes are acidic (Dos Santos Ferreira et al. 2012). The cells were plated at a concentration of T98G (29,000 cells/well) and GBM11 cells (82,000 cells/well) in 6-well plates followed by rh-SHH and/or GANT-61 treatment. After 48 h or 8 days of incubation, the cells were washed with 1×PBS and incubated with AO (3.0 μg/mL/well) in the dark for 15 min at room temperature. To quantify the percentage of cells with AVOs, they were analyzed by flow cytometry at 530/40 nm (FL1-channel-green viable cells) and 613/20 nm (FL3 channel-AVOs) (CyAn ADP flow cytometer, Beckman-Coulter, CA, USA), as described previously (Pereira et al. 2015). In three independent experiments, the mean fluorescence intensity from 10,000 events was analyzed using Summit v4.3 software (Beckman-Coulter, CA, USA) as the percentage of a cell population in each condition (viable cells, autophagic cells (AVOs positive) or unlabeled/dead cells).

Statistical Analysis

All values were expressed as mean ± SD. Groups were compared by the One-way ANOVA test or Two-way ANOVA and Tukey post-test or Bonferroni post-test, with a significance threshold of $p \leq 0.05$. All statistical analyses were performed using GraphPad Prism software (GraphPad Software Inc., San Diego, CA, USA). All experiments were done at least in three independent experiments.

Results

Different GBM Responses to SHH Signaling Modulation

Previous studies have demonstrated that GANT-61 is able to modulate components of the SHH-GLI signaling pathway, and that SHH signaling pathway stimulation usually has positive feedback on some members of the pathway (Fu et al. 2013b; Tong et al. 2018). Here we evaluate if rh-SHH or GANT-61 molecules could modulate the SHH pathway in GBM cells. To this end, the T98G and GBM11 cells were treated for 8 days with rh-SHH (2 ng/mL) or with GANT-61 (20 μM). By immunofluorescence (IF), we observed a significant increase of SHH levels in both cell lines after rh-SHH treatment compared to control (64.73% for GBM11 and 97.79% for T98G). The same was observed when we compared rh-SHH treatment to inhibited cells with GANT-61 (90.22% for GBM11 and 87.89% for T98G). The results were corroborated with the protein levels of SHH by WB (127.5% for GBM11 and 126.0% for T98G treated with rh-SHH and 168.3% for GBM11 and 127.6% for T98G treated with GANT-61) (Fig. 1a, b, g–l).

Moreover, we analyzed the PTCH1 receptor levels by IF, WB, and qRT-PCR (Fig. 1c, d, g–l). GBM11 cells treated with rh-SHH demonstrated a significant decrease of PTCH1 levels compared to GANT-61 treatment (97.85%; 35.22%, for IF and WB, respectively) (Fig. 1g–j) which was accompanied by a reduction on PTCH1 mRNA levels (65%) (Figure m). On the other hand, PTCH1 levels increased in T98G-treated conditions (Figure h and k). However, we observed a significant increase in PTCH1 levels in T98G cells treated with rh-SHH, compared to control only by WB (83.06%) (Fig. 1 k, l). While in the GANT-61-treated T98G cells it suggests stimulation of the mRNA PTCH1 levels, as we observed in GBM11-treated cells, but it was not significant compared to control (Fig. 1m, n).

Since GANT-61 exerts GLI1 effects by preventing DNA binding, its expression was evaluated (Fig. 1e–h). Our results demonstrated that rh-SHH stimulation in both cell lines resulted in an increased GLI1 nuclear levels as compared to control and GANT-61 conditions (51.17% to control and 58.28% to GANT-61 for GBM11 cells; 43.20% to control and 47.21% to GANT-61 for T98G cells) (Fig. 1e–h). However, we observed no significant differences in mRNA GLI1 levels on both cell lines, despite the appearance of an increase in GANT-61-treated T98G cells (Fig. 1m, n).

Indeed, the co-receptor SMO is inhibited by PTCH1 when the SHH signaling is activated. Here, we analyzed the expression of SMO in GBM cells by qRT-PCR. We
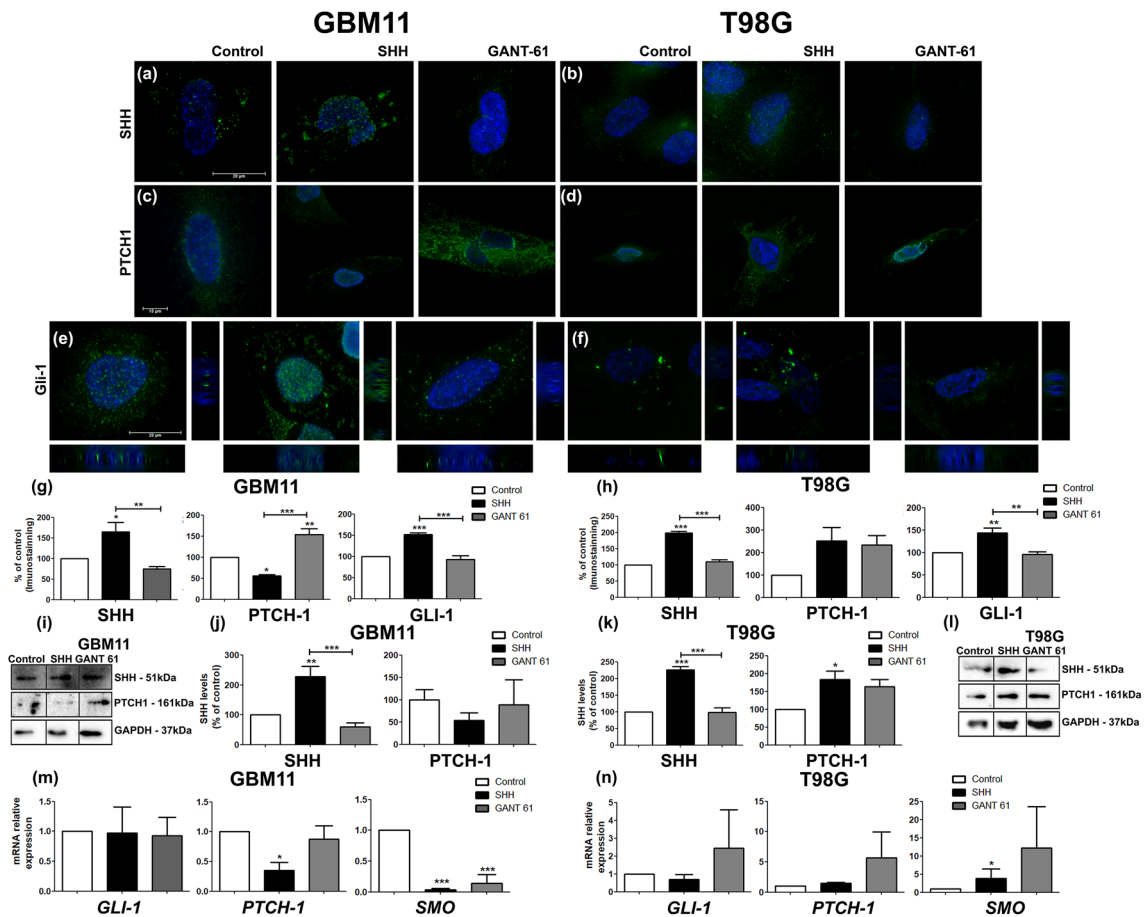
Fig. 1 rh-SHH modulates the expression of SHH, PTCH1, and GLI1 in GBM cells. GBM11 and T98G cell lines were incubated with 0.4% DMSO (control), rh-SHH (2 ng/mL), or GANT-61 (20 μM) for 8 days. **a, b** The expression profile of SHH protein for GBM11 and T98G cell lines, and **g, h** quantification of SHH-positive cells by immunofluorescence. We observed a significant increase in SHH staining when the cells were treated with rh-SHH; however, there was no significant difference when the cells were treated with GANT-61 as compared to control conditions. **c, d** The expression profile of PTCH1 protein for GBM11 and T98G cell lines, and **g, h** quantification of PTCH1-positive cells by immunofluorescence. We observed a significant decrease in SHH when the cells were treated with rh-SHH and a significant increase when the cells were treated with GANT-61 in GBM11; however, we did not observe any significant difference when T98G cells were treated with rh-SHH or GANT-61 as compared to control conditions. **e–f** The expression profile of GLI1 protein for GBM11 and T98G cell lines, and **g, h** quantification of GLI1-positive cells by immunofluorescence. We observed a significant increase in GLI1 when the cells were treated with rh-SHH; however, there was no significant difference when the cells were treated with GANT-61 as compared to control conditions. The SHH and

PTCH1 protein in GBM11 and T98G treated for 8 days were evaluated by western blotting (**i, l**). The densitometry analysis of SHH and PTCH1 in GBM-treated cells as compared to control conditions (**j, k**). We observed a significant increase in SHH when GBM11 and T98G cells were treated with rh-SHH; however, there was no significant difference when both cell lines were treated with GANT-61 as compared to control conditions (**j, k**). We also observed a significant increase in PTCH1 when T98G cells were treated with rh-SHH; however, there was no significant difference when both cell lines were treated with GANT-61 as compared to control conditions (**j, k**). The relative amount of GLI1, PTCH1, and SMO mRNA was evaluated in GBM11 and T98G cells after 8 days of treatment (**m, n**). We observed a significant decrease in PTCH1 and SMO relative amount of mRNA when GBM11 cells were treated with rh-SHH and only of SMO in T98G cells. In the GBM11 cell line we also observed a significant decrease in SMO relative amount of mRNA when GBM11 was treated with GANT-61 as compared to control conditions (**m, n**). All the mean values are derived from three independent experiments (*$P < 0.05$; **$P < 0.01$ and ***$P < 0.001$). Scale bar corresponds to 20 μm for **a, b, e** and **f**, and scale bar corresponds to 15 μm for **c** and **d**

demonstrated a significant decrease in the mRNA SMO levels in both treatments in GBM11 cells (96.84% for rh-SHH and 85.75% for GANT-61) (Fig. 1m). T98G cells stimulated with rh-SHH presented a significant increase in mRNA SMO levels (284.62%) followed by an

increasing trend (83.27%) in inhibited cells compared to the control condition (Fig. 1n). Thus, rh-SHH or GANT-61 modulates differently the expression of the molecules that regulate the SHH pathway in different GBM cell lines.

SHH Signaling Activation Supports CSC Maintenance

CSCs can initiate tumorigenesis due to their properties of self-renew and chemo- and radioresistance which are essential for the maintenance of the tumor mass in many types of cancer, such as GBMs (Lathia et al. 2015). Several studies demonstrated that SHH signaling is crucial for CSC differentiation, self-renewal, and tumorigenic potential (Balbuena et al. 2011; Goffart et al. 2013; Fu et al. 2013b). Thus, we evaluated the stem cell markers in GBM cells in the presence of rh-SHH or GANT-61. Both cell lines showed nuclear staining for the major stem cell markers: NANOG (Fig. 2a, b), OCT-4 (Fig. 2d, e) and SOX-2 (Fig. 2i, j). We observed a significant increase in NANOG nuclear staining in GBM11 cells stimulated by rh-SHH, compared to control and GANT-61 (439.893% and 488.2%, respectively) (Fig. 2c), but no significant differences were observed in T98G cells at the same conditions (Fig. 2c). On the other hand, we observed an increase in nuclear staining for OCT-4 in both cell lines treated with rh-SHH or GANT-61 (Fig. 2f) (T98G: rh-SHH, 123.8%, compared to control; 132.0%, compared to GANT-61) (Fig. 2f). Our findings were corroborated by WB analysis (GBM11: rh-SHH 58.27% and GANT-61 67.58% both compared to control) (Fig. 2g, h). For SOX-2, we observed a significant increase in nuclear staining only in rh-SHH-treated T98G cells compared to control (116.61%) (Fig. 2j, k). Similar results were observed by WB (30.04% increase for rh-SHH compared to control and 28.95% decrease for GANT-61 for T98G compared to rh-SHH) (Fig. 2l, m). Even though different GBM cell lines, our results showed the crucial role played by the SHH signaling for the maintenance of the CSC phenotype through the significant alterations in levels of those transcription factors.

SHH Stimulation Enhances Vimentin Expression in GBM Cells

EMT is important to sustain metastatic growth and has been correlated with the presence of CSCs (Fu et al. 2013b). It has been shown that SHH signaling is involved in EMT by inducing cell motility, migration, and invasion, processes in which vimentin plays a pivotal role (Kasper et al. 2006; Fu et al. 2013a). We observed increased expression of vimentin after rh-SHH treatment in both cell lines, compared to control and GANT-61 (60.77% for GBM11 and 47.87% for T98G compared to control) (Fig. 3a–d). Similar results were observed for vimentin levels by WB, being 118.51% increase for GBM11 and 58.27% increase for T98G cells stimulated with rh-SHH compared to control (Fig. 3e–g). It is interesting to note that we observed a significant decrease in vimentin levels on T98G cells treated with GANT-61 (34.94%) compared to the control condition (Fig. 3e–g). So,

our results demonstrated that SHH is involved in the EMT phenotype in GBM cell lines.

GANT-61 Modulates Cell Viability of GBM Cell Lines and Proliferation

SHH signaling pathway is crucial for tumorigenesis and its inhibition with GANT-61 interferes with tumor cell growth (Benvenuto et al. 2016). The GBM cells were treated with GANT-61 and rh-SHH for 48 h and 8 days and the cell viability was evaluated (Fig. 4). Taking into consideration that we did not observe any difference in cell viability at 48 h (Fig. 4a, b), we performed a DNA fragmentation assay by flow cytometry. The percentage of cells in sub-G_0/G_1 was less than 15% in all conditions, resulting in no significant cell population at the late cell death stage (Fig. 4c, d). Nonetheless, after 8 days of treatment with GANT-61 (Fig. 4e–h), T98G cells presented a significant decrease in cell viability (54.91%) compared to control (Fig. 4h). This result was in accordance with the results obtained from MTT assay performed with T98G cells treated with GANT-61 after 8 days of treatment (30.44% total of the nucleus compared to control condition) (Fig. 4i, j). On the other hand, no significant differences were observed in GBM11 cell viability, demonstrating their treatment resistance on both times, 48 h and 8 days.

The SHH pathway controls the proliferation of several cell types during embryogenesis and tumorigenesis. Moreover, aberrant reactivation of the SHH pathway can modulate cell growth and cancer progression, by controlling several oncogenes (Tong et al. 2018). Immunostaining for Ki-67 was performed to evaluate the effect of rh-SHH and GANT-61 in GBM proliferation (Fig. 5a). The results revealed a significant increase of Ki-67-positive cells after 8 days of treatment with rh-SHH on both cell lines (46.68% for GBM11 and 101.06% for T98G compared to control) (Fig. 5b, c). However, we did not observe any differences in both GBM cells treated with GANT-61, suggesting no cytostatic effect of GANT-61 (Fig. 5b, c). These findings were confirmed by flow cytometry, where no significant arrest in any phase of the cell cycle in GBM11 or T98G cell lines was observed (Fig. 5d, e).

The downstream effectors of SHH signaling pathway, GLI1, and GLI2 regulate proliferation factors such as MYC, Cyclin E, Cyclin D1, prosurvival protein BCL-2, the GLI transcription factors themselves, and PTCH1 (Katoh and Katoh 2005; Lee et al. 2007; Mazumdar et al. 2011; McKee et al. 2012). To investigate if rh-SHH and GANT-61 could modulate c-MYC in GBM cells, WB analysis was performed (Fig. 5f–h). We observed a significant increase of c-MYC protein levels on both GBM cell lines treated with rh-SHH (GBM11: 53.47% and T98G cells: 32.85%), compared to control (Fig. 5f, g). In the GBM11 cells treated with
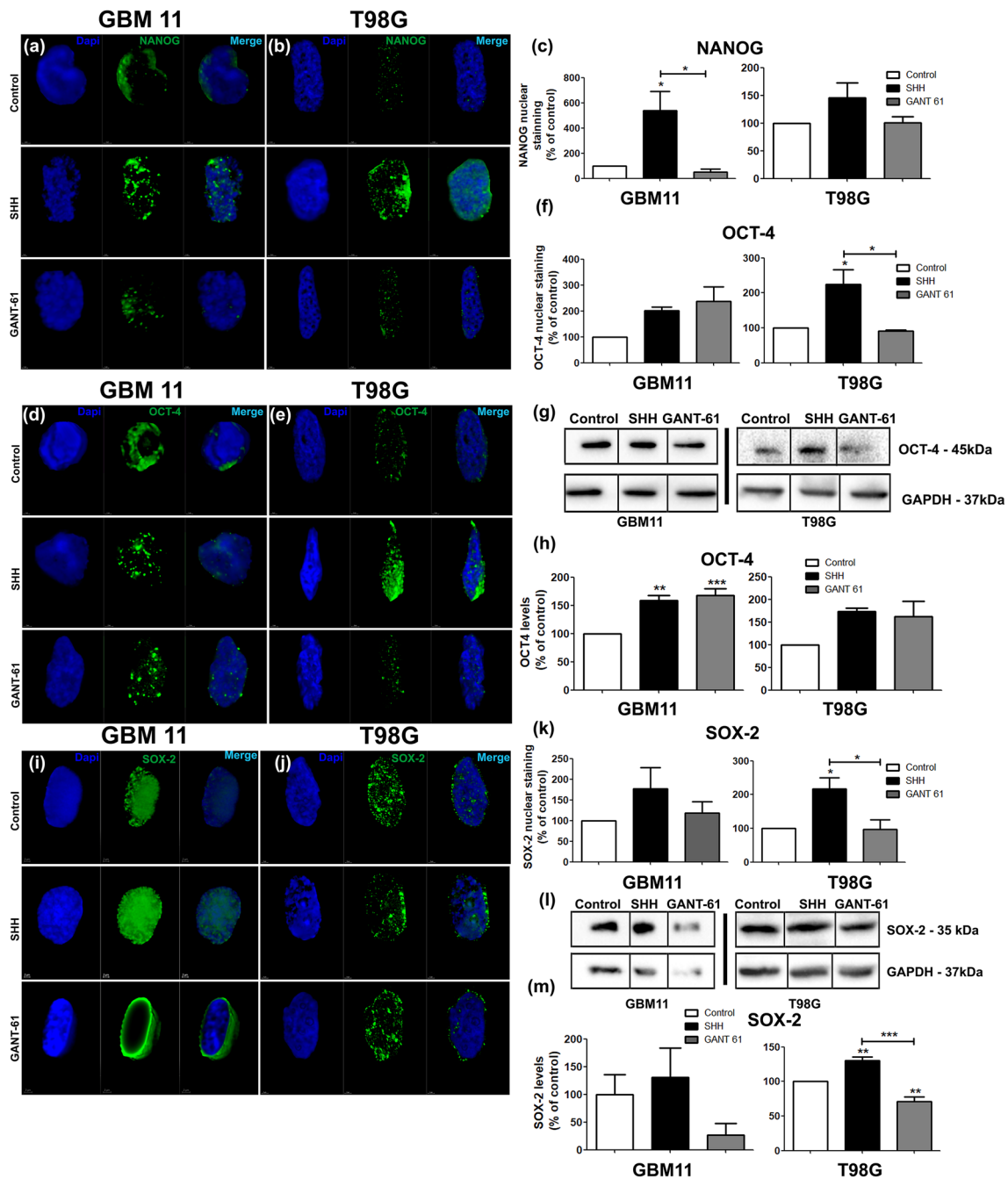
Fig. 2 GANT-61 and rh-SHH modulates the expression of NANOG, OCT-4, and SOX-2 in GBM cells. GBM11 and T98G cell lines were incubated with 0.4% DMSO (control), rh-SHH (2 ng/mL), or GANT-61 (20 μM) for 8 days. **a**, **b** The expression profile of NANOG protein for GBM11 and T98G cell lines, and **c** quantification of NANOG-positive cells by immunofluorescence. We observed a significant increase in NANOG staining when the cells were treated with rh-SHH; however, there was no significant difference when the cells were treated with GANT-61 as compared to control conditions. **d**, **e** The expression profile of OCT-4 protein for GBM11 and T98G cell lines, and **f** quantification of OCT-4-positive cells by immunofluorescence. We observed a significant increase in OCT-4 when T98G cells were treated with rh-SHH; however, there was no significant difference when both were treated with GANT-61 as compared to control conditions. The OCT-4 protein in GBM11 and T98G treated for 8 days was evaluated by western blotting (**g**). The densitometry analysis of OCT-4 in GBM-treated cells as compared to control conditions (**h**). We observed a significant increase in OCT-4 when GBM11 cells were treated with rh-SHH or GANT-61 (**h**). **i**, **j** The expression profile of SOX-2 protein for GBM11 and T98G cell lines, and **k** quantification of SOX-2-positive cells by immunofluorescence. We observed a significant increase in SOX-2 staining when T98G cells were treated with rh-SHH; however, there was no significant difference when both were treated with GANT-61 as compared to control conditions. The SOX-2 protein in GBM11 and T98G treated for 8 days was evaluated by western blotting (**l**). The densitometry analysis of SOX-2 in GBM-treated cells as compared to control conditions (**m**). We observed a significant increase in SOX-2 when T98G cells were treated with rh-SHH and a significant decrease when T98G cells were treated with GANT-61 as compared to control conditions (**m**). All the mean values are derived from three independent experiments (*$P < 0.05$; **$P < 0.01$ and ***$P < 0.001$). Scale bar corresponds to 2 μm
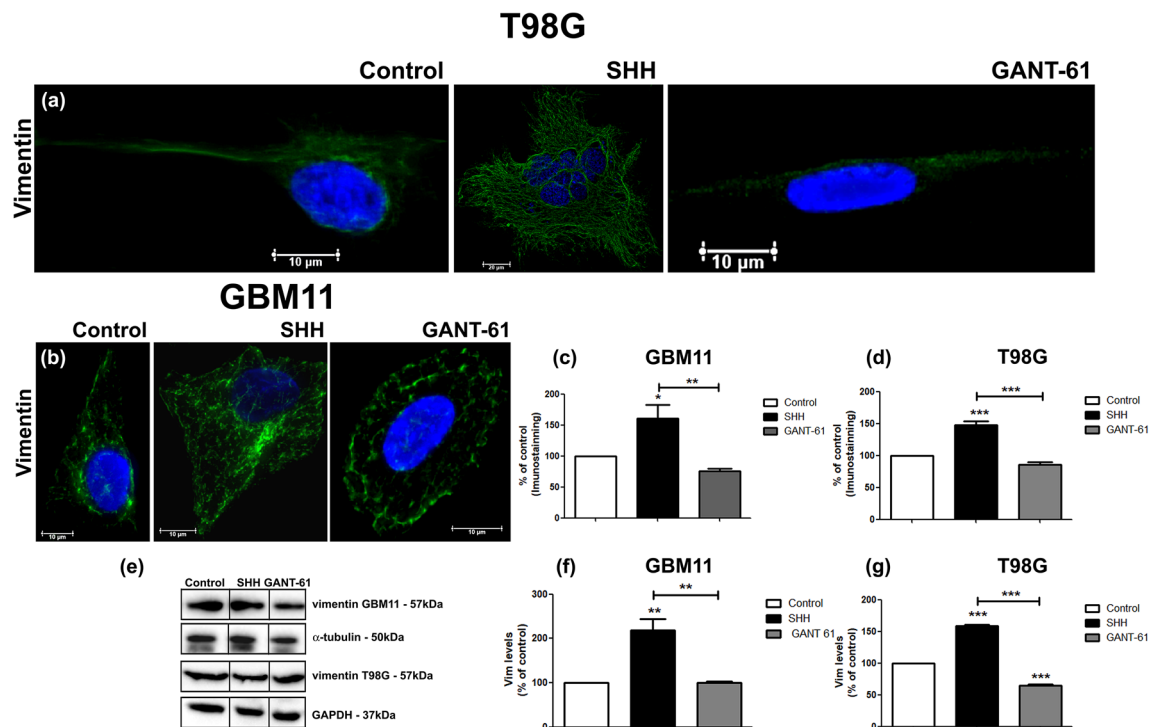
Fig. 3 rh-SHH induces epithelial-mesenchymal transition on GBM cell lines. GBM11 and T98G cell lines were incubated with 0.4% DMSO (control), rh-SHH (2 ng/mL), or GANT-61 (20 µM) for 8 days. **a**, **b** The expression profile of vimentin protein for GBM11 and T98G cell lines, and **c**, **d** quantification of vimentin-positive cells by immunofluorescence. We observed a significant increase in vimentin when the cells were treated with rh-SHH; however, there was no significant difference when the cells were treated with GANT-61 as compared to control conditions. The vimentin protein in GBM11 and T98G treated for 8 days was evaluated by western blotting (**e**). The densitometry analysis of vimentin in GBM-treated cells as compared to control conditions (**f**, **g**). We observed a significant increase in vimentin when both cell lines were treated with rh-SHH and a significant decrease when T98G cells were treated with GANT-61 as compared to control conditions (**f**, **g**). All the mean values are derived from three independent experiments (*$P < 0.05$; **$P < 0.01$, and ***$P < 0.001$). Scale bar corresponds to 10 or 20 µm (for T98G SHH)

GANT-61, c-MYC levels were reduced by 29.42% compared to control cells (Fig. 5f, h).

c-MYC is a transcriptional target of miR-17−92 cluster family (Mendell 2008) which usually is overexpressed upon abnormal SHH signaling activation during medulloblastoma formation (O'Donnell et al. 2005; Uziel et al. 2009a). Thus, we investigated the expression of miR-17-5p, a member of the miR-17−92 cluster family (Mendell 2008; Uziel et al. 2009b; Kefas et al. 2009; Zindy et al. 2014). The results showed high miR-17-5p levels in GBM11 and T98G cells, compared to human healthy astrocytes (Fig. 5i). Moreover, GBM11 cells stimulated with rh-SHH induced the expression of miR-17-5p by 11% compared to inhibited cells with GANT-61 (Fig. 5i).

On the other hand, miR-326 is usually down-regulated in gliomas, by acting as a negative regulator for SHH pathway through directly targeting SMO and Gli2 (Jiang et al. 2014a; Du et al. 2015). Thus, the expression of miR-326 was investigated in GBM cells. We observed down-regulation of miR-326 levels in both cell lines compared to human astrocytes; however, we did not observe any difference in its expression after 8 days of treatment with rh-SHH or GANT-61 (Fig. 5 j).

GANT-61 Induces Autophagy and Apoptosis in GBM Cell Lines

It was already described that GANT-61 induces different cellular mechanisms as autophagy and apoptosis (Wang et al. 2018). GBM cells were treated with GANT-61 for 8 days and the LC3-II expression, an autophagy marker, was analyzed by WB. The results showed an increase of GANT-61-induced autophagy by up-regulation of LC3-II levels in GBM11 cells (Fig. 6a). We also observed the presence of acidic vacuoles (AVOs) by flow cytometry in GBM11 cells treated with GANT-61, compared to control (32.03%) or rh-SHH (29.96%) (Fig. 6b). However, T98G cells showed a low bandwidth of LC3 II, which corroborates the results obtained in AVOs formation (Fig. 6c). Autophagy was also confirmed by the inhibition of p70-S6K, a member of the mTOR signaling pathway that affects cell proliferation, growth, metabolism, and survival (Laplante and Sabatini
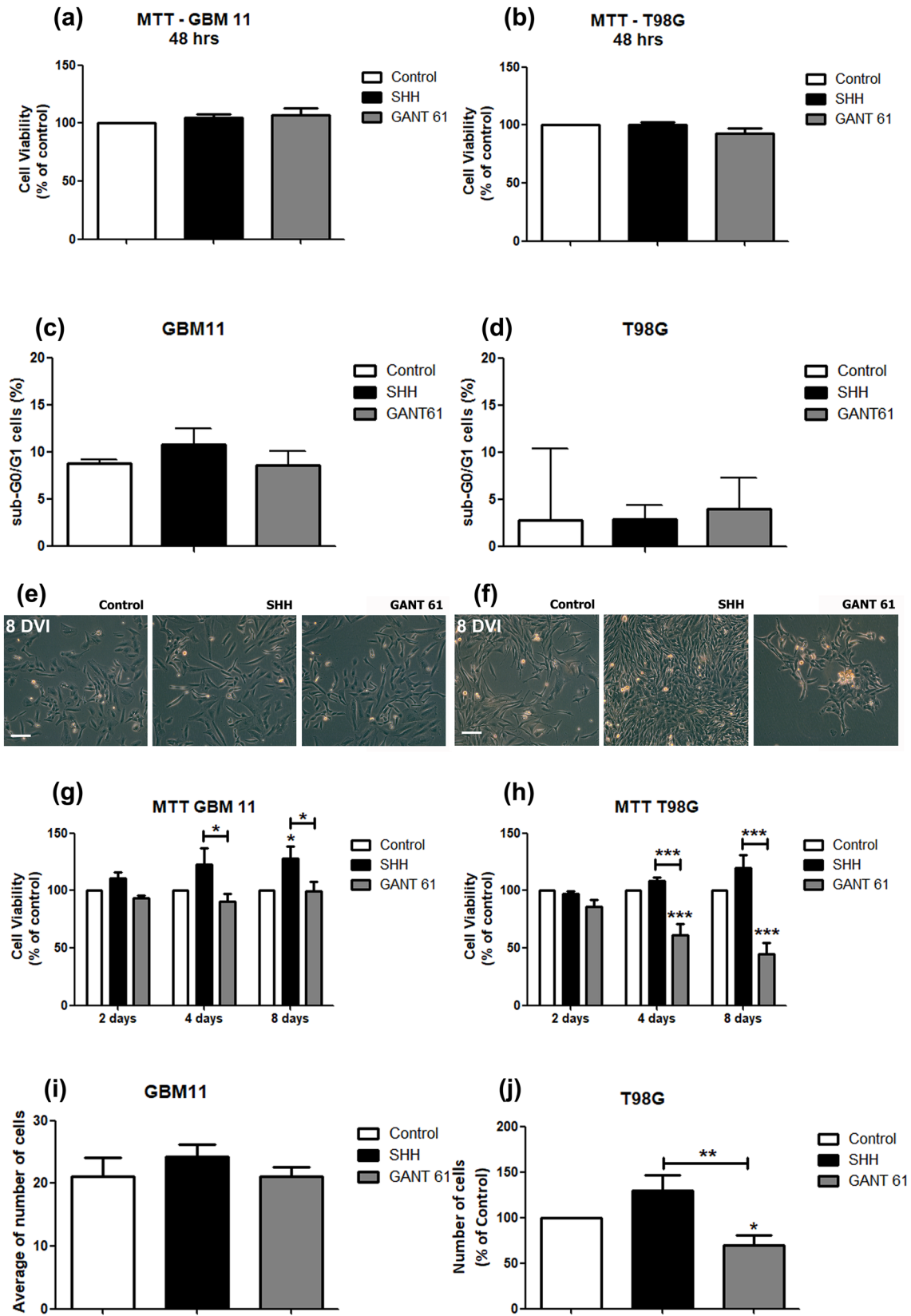
◀**Fig. 4** GBM11 and T98G presented a different viability response to GANT-61. GBM11 and T98G cell lines were incubated with 0.4% DMSO (control), rh-SHH (2 ng/mL), or GANT-61 (20 μM). The MTT assay was performed after 48 h (**a**, **b**) of treatment. Percentage of total cells in the sub-G_0/G_1 phase after 48 h of treatment by flow cytometry (**c**, **d**). GBM11 and T98G cells observed using phase-contrast microscopy after 8 days of treatment with rh-SHH (2 ng/mL) or GANT-61 (20 μM) (**e**, **f**). GBM11 and T98G were treated for 8 days and then the MTT assay was performed. GANT-61 induces a reduction in T98G cell viability; however, GBM11 was not affected by GANT-61 treatment (**g**, **h**). After 8 days of treatment, we counted the positive cells for DAPI through fluorescence microscopy (**i**, **j**). All the mean values are derived from three independent experiments. The decrease in cell viability was analyzed comparing all conditions to the control condition. (*$P < 0.05$). Scale bar corresponds to 50 μm

2009) (Fig. 6d–f). We observed a significant decrease of p70-S6K in GANT-61 condition, in both cell lines compared to control (GBM11: 62.63% and T98G: 40.16%) (Fig. 6e, f). Autophagy can modulate cell death mechanisms, and especially apoptosis, by degrading cellular components that can induce the cell to activate the apoptosis machinery (Gump and Thorburn 2011). We thus investigated the effect of SHH inhibition in GBM cells by evaluating the levels of procaspase 9, cleaved caspase 9, and activated caspase 3 by WB. Both cell lines demonstrated an increased level of cleaved caspase 9 after the treatment of GANT-61 for 8 days compared to control (Fig. 6g). Moreover, the activated caspase 3 was increased in both GBM cell lines inhibited by GANT-61 compared to control (GBM11: 40.97% and T98G: 49.71%) (Fig. 6h–j). Thus, GANT-61 treatment enhanced autophagy and apoptosis of GBM cell lines.

Discussion

In the present work, we investigated the effect of GANT-61 and rh-SHH in GBM cell lines. We demonstrated that SHH inhibition with GANT-61 induced autophagy on GBM cell lines after 8 days of treatment. We also observed apoptosis on those GBM cell lines. Moreover, when we treated the cells with rh-SHH we observed an increase in proliferation, stem cell phenotype, EMT markers, and positive feedback on the SHH pathway. Our results suggested that SHH pathway inhibition is a promising strategy to be used on resistant GBMs.

We observed by MTT assay that only T98G cells presented a significant decrease in cell viability after 8 days of treatment with GANT-61. Moreover, with the most resistant GBM cell line, GBM11, we did not observe any significant difference in cell viability by treating the cells with GANT-61 for 8 days. We believe that GANT-61 treatment could have altered the metabolic activity of GBM11 since the tetrazolium dye reduction did not affect the cell viability. It is already known that cell viability measured

by MTT-formazan reduction is dependent on mitochondrial respiration and indirectly serves to assess the cellular energy (Stockert et al. 2018). Recently, a study has demonstrated that mitochondrial metabolism enhanced autophagy in cancer cells (Thomas et al. 2018). We observed that GANT-61 induced autophagy on GBM11 cells, and maybe this could explain this result. Moreover, another possibility that we cannot rule out is the hypothesis that the SHH pathway is being activated by crosstalk with other pathways, such as WNT and transforming growth factor-beta (TGF-β), which is very common to occur in the tumor environment (Carballo et al. 2018b).

Aberrant activation of SHH signaling is very common in cancers, and ligand-independent constitutive activation of the SHH pathway was already described in medulloblastoma, basal cell carcinoma, GBMs, and breast cancer (Cao et al. 2012; Zheng et al. 2013; Zhu et al. 2014). As we did not observe any difference in cell viability when we treated GBM11 with GANT-61, we also believe that these cells could have mutations that inactivate the negative regulator SuFu (*Suppressor of Fused*) and/or hyperactivation of GLI1 (Zheng et al. 2013). Moreover, the GBM11 cell line was isolated from a patient that was submitted to radiotherapy and chemotherapy with TMZ, being this cell line IDH 1/2 and p53 wild type (Balça-Silva et al. 2017). Recently, the World Health Organization classification of tumors of the CNS described that usually, primary or de novo GBM cells (as GBM11 cell line) are IDH-wild type (about 90% of cases) (Louis et al. 2016).

It is interesting to note that GANT-61 induced autophagy and apoptosis in both cell lines. However, we observed that GANT-61 induced mainly autophagy in GBM11 cells, while apoptosis was observed mainly in T98G cells. It was already demonstrated that common upstream signals can induce both autophagy and apoptosis (Maiuri et al. 2007; Filippi-Chiela et al. 2011). In GBM cells, it was demonstrated that resveratrol, an inhibitor of the SHH pathway, acts in GLI1 by inducing apoptosis and autophagy (Filippi-Chiela et al. 2011). Similar results were observed in neuroblastoma, human chondrosarcoma cells, and non-small cell lung cancer cells, when SHH signaling pathway inhibition induced autophagy and apoptosis (Mao et al. 2009; Schiapparelli et al. 2011; Jin et al. 2014; Wang et al. 2014; Sun et al. 2014; Xu et al. 2015). GANT-61 inducing only autophagy was also observed in ovarian, gastric and colon cancer cell lines, and in hepatocellular carcinoma cells (Wang et al. 2013b; Tang et al. 2015).

Several evidences demonstrated that SHH signaling promotes cellular proliferation by opposing signals that induce physiologic growth arrest (Chen et al. 2007). Moreover, it was demonstrated that SHH inhibition can reduce proliferation in several cancers including gliomas, prostate, and pancreas (Clement et al. 2007; Fu et al. 2013b; Huang et al.
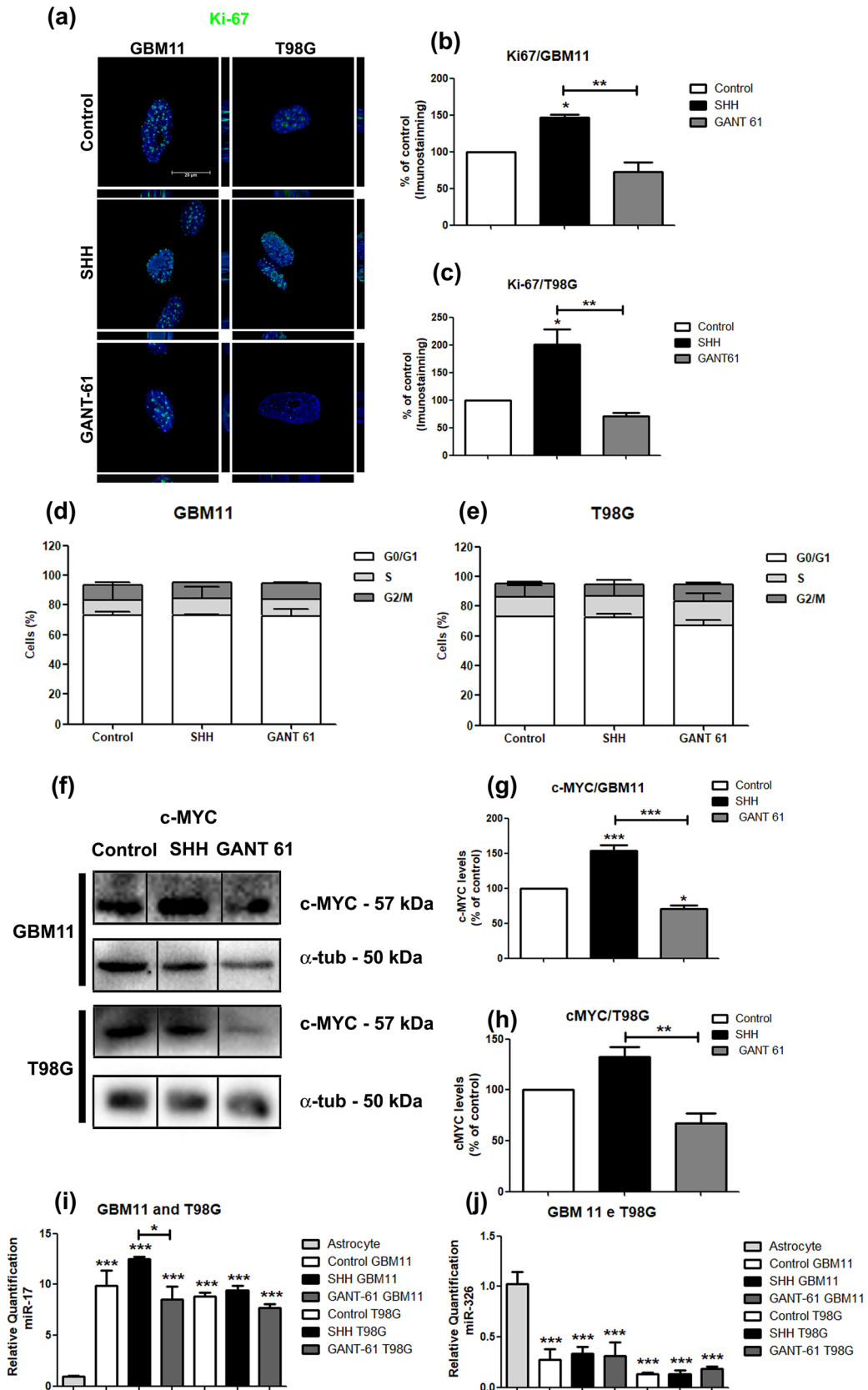
◄**Fig. 5** Ki-67 proliferation marker was not affected following treatment with GANT-61 in GBM cell lines. BM11 and T98G cell lines were incubated with 0.4% DMSO (control), rh-SHH (2 ng/mL), or GANT-61 (20 μM) for 8 days. **a** The expression profile of Ki-67 protein for GBM11 and T98G cell lines, and **b**, **c** quantification of Ki-67-positive cells by immunofluorescence. We observed a significant increase in Ki-67 staining when the cells were treated with rh-SHH; however, there was no significant difference when the cells were treated with GANT-61 as compared to control conditions. In **d**, **e**, we can observe the percentage of GBM11 and T98G cells in cell cycle phases G_0/G_1, S, and G_2/M by flow cytometry. rh-SHH or GANT-61 did not affect the percentage of cells in G_0/G_1, S, and G_2/M phases. The protein synthesis of c-MYC in GBM11 and T98G treated during 8 days was evaluated by western blotting (**f**). The densitometry analysis of c-MYC in GBM-treated cells. We observed a significant increase in c-MYC protein when GBM11 and T98G cells were treated with rh-SHH; however, there was no significant difference when both cell lines were treated with GANT-61 as compared to control conditions (**g**, **h**). The relative amount of miR-17 and miR-326 was evaluated in GBM11 and T98G cells after 8 days of treatment and compared with a non-pathological cell, the astrocyte (**i**, **j**). We observed that the GBM cells presented increased miR-17 levels compared to astrocytes; however, they also presented decreased levels of miR-326 in comparison of astrocytes. All the mean values are derived from three independent experiments ($*P < 0.05$; $**P < 0.01$ and $***P < 0.001$)

2014). However, we did not observe any alteration in proliferation when the cells were treated with GANT-61. These results could be explained by intrinsic heterogeneity present in GBM cells or the time point that was chosen to treat the cells. On the other hand, our findings showed that rh-SHH induced proliferation in both cells, as expected. The activation of GLI1 with rh-SHH can also positively induce proliferation through direct transcriptional up-regulation of c-MYC as we observed (Di Magliano and Hebrok 2003). Moreover, SHH pathway can be controlled by several miRNAs, such as miR-17 and miR-326 (Uziel et al. 2009a; Jiang et al. 2014a). When we compared the relative amount of miR-17 with healthy glial cells, the astrocytes, we observed that GBM11 presented an increase of tenfold of miR-17 expression. miR-17−92 cluster family is a downstream target of c-MYC which interacts with SHH signaling in medulloblastoma formation (O'Donnell et al. 2005; Uziel et al. 2009a). Regarding the low expression of miR-326, a tumor suppressor, in gliomas and its role in proliferation and apoptosis (Wang et al. 2013a; Du et al. 2015), we investigated if the expression of miR-326 in GBM cells could explain the alterations observed in proliferation, as we believed that this miRNA could be down-regulated in GBM cell lines studied here. We observed that GBM cells expressed threefold less miR-326, compared to healthy astrocytes. It has been already reported that miR-326 acts as a negative regulator for the SHH pathway by directly targeting SMO and GLI2 (Jiang et al. 2014b), so the over-expression of miR-326 with curcumin, for instance, could decrease SHH/GLI1 activity and therefore being a promising therapeutic agent for GBM (Yin et al. 2016).

It is well established that the cellular response of the SHH signal depends on both levels of individual GLI genes expressed and the level of SHH secreted. When GLI translocates to the nucleus it activates target genes, including *GLI1* and *PTCH1* in positive and negative feedback, respectively (Blotta et al. 2012). When we treated GBM cells with rh-SHH, we observed positive feedback of the SHH signaling pathway since we observed an increase in SHH and GLI1 expression. However, in the rh-SHH-treated T98G cells, we observed an increase in PTCH1 expression. Moreover, on both cell lines, we observed an increase of PTCH1 expression after GLI inhibition with GANT-61. Our results corroborate with a previous work, which demonstrated a mixed expression pattern of PTCH1 among the low-grade to high-grade samples of astrocytoma tumor samples analyzed. Some high-grade tumors expressed high levels of PTCH1 when GLI1 was silenced, and one of them was the T98G cell line (Shahi et al. 2010). We cannot discard the hypothesis that high PTCH1 levels after GANT-61 treatment was due to the receptor translocation to the membrane. This could be happening in an attempt to maintain the pathway active, inducing tumorigenesis. Although PTCH is usually a tumor suppressor, it was demonstrated that the over-expression of *Ptch1* induces alternative epidermal cell fate decisions leading to increased squamous cell carcinoma formation (Kang et al. 2013). Treating GBM11 with GANT-61 we observed a significant decrease in *SMO* mRNA probably inducing a more prominent inhibition of the pathway.

Besides activating *GLI1* and *PTCH1*, when GLI1 translocates to the nucleus it also activates genes that are important for stemness state, such as SOX-2, OCT-4, and NANOG. It has been demonstrated that GANT-61 can inhibit the expression of pluripotency maintenance factors (Fu et al. 2013b). Here, we observed that GBM cells treated with rh-SHH increased the expression of pluripotency factors as NANOG, OCT-4 and SOX-2, as expected. However, in the presence of GANT-61, we also observed an increased expression of OCT-4. As we showed, GANT-61 treatment induces death, which could explain these results since there were only fewer cells in the culture suggesting that the cells left were stem cells. However, this is still under investigation.

Glioblastomas usually spread quickly and invade other parts of the brain, making complete surgical removal more difficult. Moreover, EMT is important to sustain metastatic growth that is crucial for CSC dissemination and resistance (Mittal 2018). Lastly, we observed that rh-SHH increased vimentin expression on both cell lines suggesting that SHH signaling can induce EMT phenotype. Several reports demonstrated that EMT is important for metastasis and that SHH signaling also acts in CSCs by inducing EMT phenotype (Shahi et al. 2012; Fu et al. 2013a). The GANT-61-treated cells did not present any modifications in vimentin expression, although some reports have already demonstrated that
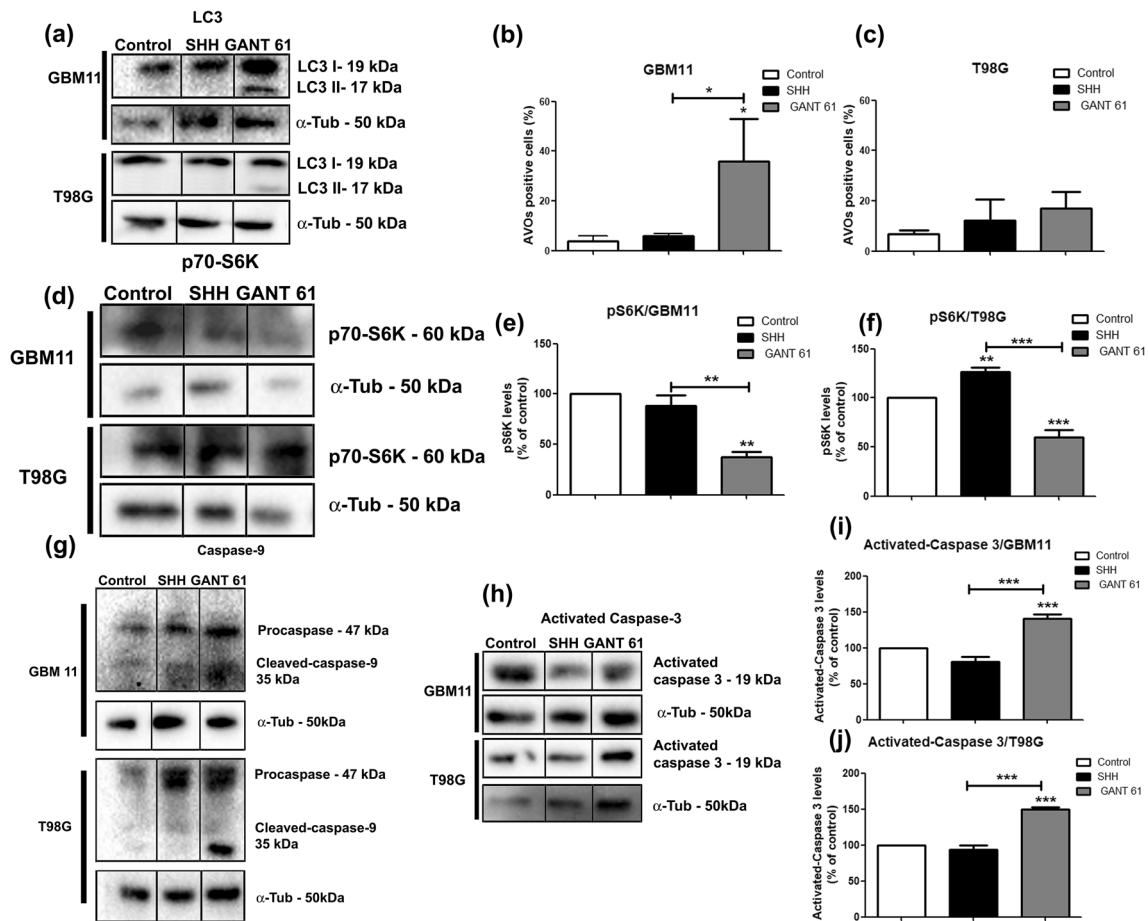
Fig. 6 GANT-61 induces autophagy and apoptosis in GBM cell lines. GBM11 and T98G cell lines were incubated with 0.4% DMSO (control), rh-SHH (2 ng/mL), or GANT-61 (20 μM) for 8 days. The LC3-I and LC3-II protein in GBM11 and T98G treated for 8 days were evaluated by western blotting (**a**). Acidic vesicles (AVOs) were determined by flow cytometry. GANT-61 increased AVOs GBM11 and T98G cells, which was statistically significant to GBM11 (**b**, **c**). The p70-S6K in GBM11 and T98G treated for 8 days were evaluated by western blotting (**d**). We observed a significant increase in p70-S6K protein when the T98G cell line was treated with rh-SHH and a significant decrease when both cell lines were treated with GANT-61 as compared to control conditions (**e–f**). The procaspase 9, cleaved caspase 9, and activated caspase-3 protein in GBM11 and T98G treated for 8 days were evaluated by western blotting (**g–h**). We observed a significant increase in cleaved caspase 9 and activated caspase 3 when both cell lines were treated with GANT-61 as compared to control conditions (**i–j**). All the mean values are derived from three independent experiments (*$P < 0.05$; **$P < 0.01$ and ***$P < 0.001$)

GANT-61 can inhibit EMT (Fu et al. 2013b; Ke et al. 2015; Amantini et al. 2016).

In conclusion (Fig. 7), when SHH is present, the pathway is active and the receptor PTCH1 does not repress the co-receptor SMO, initiating the signaling pathway. Then, SUFU that is the negative regulator of the pathway releases GLI transcription factor which translocates to the nucleus activating target genes, such as SHH, GLI1, OCT-4, SOX-2, NANOG, and vimentin, responsible for proliferation, migration, and cell survival. By targeting GLI using GANT-61, we observed an increase in the proteins that are involved with autophagy and apoptosis, such as LC3 II and cleaved

caspases 9 and 3, respectively. Therefore, selective inhibition of the SHH pathway could be an important tool to assist in the treatment of patients suffering from GBMs refractory to gold standard treatment (Honorato et al. 2020). Here, we highlighted the importance of SHH signaling pathway inhibition regarding GBM resistance and its heterogeneity. We have used two different GBM primary cell lines that have responded differently to SHH inhibition. This reinforces that personalized medicine would be pivotal for the best therapeutic approach to the patients, concerning the different GBM phenotypes.
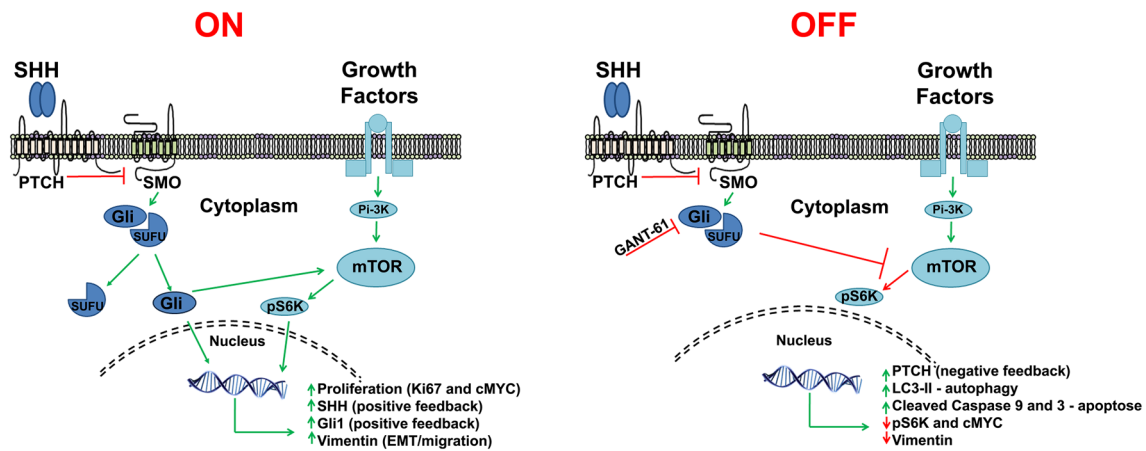
Fig. 7 Scheme of GANT-61 and rh-SHH action in GBM cell lines. When SHH is present, the pathway is active and the receptor PTCH1 does not repress the co-receptor SMO, initiating the signaling pathway. When this happens, SUFU that is the negative regulator of the pathway releases GLI transcription factor that translocates to the nucleus activating target genes, such as SHH, GLI1, OCT-4, SOX-2, NANOG, and vimentin that are responsible for proliferation, migration, and cell survival. When the pathway is inhibited with GANT-61 at GLI, we observe an increase in the proteins that are involved with cell death, such as LC3 II and cleaved caspases 9 and 3, inducing apoptosis and autophagy on those cell lines

Compliance with Ethical Standards

References

Amantini C, Morelli MB, Nabissi M et al (2016) Capsaicin triggers autophagic cell survival which drives epithelial mesenchymal transition and chemoresistance in bladder cancer cells in an Hedgehog-dependent manner. Oncotarget. https://doi.org/10.18632/oncotarget.10326

Bailey JM, Singh PK, Hollingsworth MA (2007) Cancer metastasis facilitated by developmental pathways: sonic hedgehog, notch, and bone morphogenic proteins. J Cell Biochem 102:829–839. https://doi.org/10.1002/jcb.21509

Balbuena J, Pachon G, Lopez-Torrents G et al (2011) ABCG2 is required to control the sonic hedgehog pathway in side population cells with stem-like properties. Cytom Part A 79A:672–683. https://doi.org/10.1002/cyto.a.21103

Balça-Silva J, Matias D, Dubois LG et al (2017) The Expression of Connexins and SOX2 Reflects the Plasticity of Glioma Stem-Like Cells. Transl Oncol 10:555–569. https://doi.org/10.1016/j.tranon.2017.04.005

Benvenuto M, Masuelli L, De Smaele E et al (2016) In vitro and in vivo inhibition of breast cancer cell growth by targeting the Hedgehog/GLI pathway with SMO (GDC-0449) or GLI (GANT-61) inhibitors. Oncotarget. https://doi.org/10.18632/oncotarget.7062

Blotta S, Jakubikova J, Calimeri T et al (2012) Canonical and non-canonical hedgehog pathway in the pathogenesis of multiple myeloma. Blood 120:5002–5013. https://doi.org/10.1182/blood-2011-07-368142

Bonavia R, Inda MM, Cavenee WK, Furnari FB (2011) Heterogeneity maintenance in glioblastoma: a social network. Cancer Res 71:4055–4060. https://doi.org/10.1158/0008-5472.CAN-11-0153

Bray F, Ferlay J, Soerjomataram I et al (2018) Global cancer statistics 2018: GLOBOCAN estimates of incidence and mortality worldwide for 36 cancers in 185 countries. CA Cancer J Clin. https://doi.org/10.3322/caac.21492

Cao X, Geradts J, Dewhirst MW, Lo HW (2012) Upregulation of VEGF-A and CD24 gene expression by the tGLI1 transcription

factor contributes to the aggressive behavior of breast cancer cells. Oncogene 31:104–115. https://doi.org/10.1038/onc.2011.219

Carballo GB, Honorato JR, De Lopes GPF, Spohr TCLDS (2018a) A highlight on Sonic Hedgehog Pathway. Cell Commun Signal 16:11

Carballo GB, Honorato JR, De Lopes GPF, Spohr TCLDSE (2018b) A highlight on Sonic hedgehog pathway. Cell Commun Signal 16:1–15. https://doi.org/10.1186/s12964-018-0220-7

Chen X, Horiuchi A, Kikuchi N et al (2007) Hedgehog signal pathway is activated in ovarian carcinomas, correlating with cell proliferation: it's inhibition leads to growth suppression and apoptosis. Cancer Sci 98:68–76

Clement V, Sanchez P, de Tribolet N et al (2007) HEDGEHOG-GLI1 signaling regulates human glioma growth, cancer stem cell self-renewal, and tumorigenicity. Curr Biol 17:165–172. https://doi.org/10.1016/j.cub.2006.11.033

Dahmane N, Lee J, Robins P et al (1997) Activation of the transcription factor Gli1 and the Sonic hedgehog signalling pathway in skin tumours. Nature 389:876–881. https://doi.org/10.1038/39918

Dean M, Fojo T, Bates S (2005) Tumour stem cells and drug resistance. Nat Rev Cancer 5:275–284. https://doi.org/10.1038/nrc1590

Di Magliano MP, Hebrok M (2003) Hedgehog signalling in cancer formation and maintenance. Nat Rev Cancer 3:903–911

Dos Santos Ferreira AC, Fernandes RA, Kwee JK, Klumb CE (2012) Histone deacetylase inhibitor potentiates chemotherapy-induced apoptosis through Bim upregulation in Burkitt's lymphoma cells. J Cancer Res Clin Oncol 138:317–325. https://doi.org/10.1007/s00432-011-1093-y

Du W, Liu X, Chen L et al (2015) Targeting the SMO oncogene by miR-326 inhibits glioma biological behaviors and stemness. Neuro Oncol 17:243–253. https://doi.org/10.1093/neuonc/nou217

Faria J, Romão L, Martins S et al (2006) Interactive properties of human glioblastoma cells with brain neurons in culture and neuronal modulation of glial laminin organization. Differentiation 74:562–572. https://doi.org/10.1111/j.1432-0436.2006.00090.x

Filippi-Chiela EC, Villodre ES, Zamin LL, Lenz G (2011) Autophagy interplay with apoptosis and cell cycle regulation in the growth inhibiting effect of resveratrol in glioma cells. PLoS ONE. https://doi.org/10.1371/journal.pone.0020849

Fu J, Rodova M, Nanta R et al (2013a) NPV-LDE-225 (Erismodegib) inhibits epithelial mesenchymal transition and self-renewal of glioblastoma initiating cells by regulating miR-21, miR-128, and miR-200. Neuro Oncol 15:691–706. https://doi.org/10.1093/neuonc/not011not011

Fu J, Rodova M, Roy SK et al (2013b) GANT-61 inhibits pancreatic cancer stem cell growth in vitro and in NOD/SCID/IL2R gamma null mice xenograft. Cancer Lett 330:22–32. https://doi.org/10.1016/j.canlet.2012.11.018S0304-3835(12)00665-9

Geraldo LHM, Garcia C, da Fonseca ACC et al (2019) Glioblastoma therapy in the age of molecular medicine. Trends Cancer 5:46–66

Goffart N, Kroonen J, Rogister B (2013) Glioblastoma-initiating cells: relationship with neural stem cells and the micro-environment. Cancers (Basel) 5:1049–1071. https://doi.org/10.3390/cancers5031049

Golestaneh N, Mishra B (2005) TGF-β, neuronal stem cells and glioblastoma. Oncogene 24:5722–5730. https://doi.org/10.1038/sj.onc.1208925

Gonnissen A, Isebaert S, McKee CM et al (2016) The hedgehog inhibitor GANT61 sensitizes prostate cancer cells to ionizing radiation both *in vitro* and *in vivo*. Oncotarget 7:84286–84298. https://doi.org/10.18632/oncotarget.12483

Gump JM, Thorburn A (2011) Autophagy and apoptosis: What is the connection? Trends Cell Biol 21:387–392. https://doi.org/10.1016/j.tcb.2011.03.007

Hanahan D, Coussens LM (2012) Accessories to the crime: functions of cells recruited to the tumor microenvironment. Cancer Cell 21:309–322

Honorato JR, Hauser-Davis RA, Saggioro EM et al (2020) Role of Sonic hedgehog signaling in cell cycle, oxidative stress, and autophagy of temozolomide resistant glioblastoma. J Cell Physiol 235:3798–3814. https://doi.org/10.1002/jcp.29274

Huang L, Walter V, Hayes DN, Onaitis M (2014) Hedgehog-GLI signaling inhibition suppresses tumor growth in squamous lung cancer. Clin Cancer Res 20:1566–1575. https://doi.org/10.1158/1078-0432.CCR-13-2195

Jiang C-L, Chen L-C, Cui Y-Q et al (2014a) Targeting glioma stem cells via the Hedgehog signaling pathway. Neuroimmunol Neuroinflamm 1:51. https://doi.org/10.4103/2347-8659.139715

Jiang Z, Cushing L, Ai X, Lu J (2014b) miR-326 is downstream of Sonic hedgehog signaling and regulates the expression of Gli2 and smoothened. Am J Respir Cell Mol Biol 51:273–283. https://doi.org/10.1165/rcmb.2013-0127OC

Jin W, Ming X, Hou X et al (2014) Protective effects of erythropoietin in traumatic spinal cord injury by inducing the Nrf2 signaling pathway activation. J Trauma Acute Care Surg 76:1228–1234

Kang HC, Wakabayashi Y, Jen K et al (2013) Ptch1 overexpression drives skin carcinogenesis and developmental defects in K14PtchFVB Mice. J Invest Dermatol 133:1311–1320. https://doi.org/10.1038/jid.2012.419

Kasper M, Regl G, Frischauf AM, Aberger F (2006) GLI transcription factors: mediators of oncogenic Hedgehog signalling. Eur J Cancer 42:437–445. https://doi.org/10.1016/j.ejca.2005.08.039

Katoh Y, Katoh M (2005) Comparative genomics on Sonic Hedgehog orthologs. Oncol Rep 14:1087–1090

Ke Z, Caiping S, Qing Z, Xiaojing W (2015) Sonic hedgehog–Gli1 signals promote epithelial–mesenchymal transition in ovarian cancer by mediating PI3K/AKT pathway. Med Oncol 32:1–9. https://doi.org/10.1007/s12032-014-0368-y

Kefas B, Comeau L, Floyd DH et al (2009) The neuronal microRNA miR-326 acts in a feedback loop with notch and has therapeutic potential against brain tumors. J Neurosci 29:15161–15168. https://doi.org/10.1523/JNEUROSCI.4966-09.2009

Kimura H, Stephen D, Joyner A, Curran T (2005) Gli1 is important for medulloblastoma formation in Ptc1+/- mice. Oncogene 24:4026–4036

Koike Y, Ohta Y, Saitoh W et al (2017) Anti-cell growth and anti-cancer stem cell activities of the non-canonical hedgehog inhibitor GANT61 in triple-negative breast cancer cells. Breast Cancer 24:683–693. https://doi.org/10.1007/s12282-017-0757-0

Kurebayashi J, Koike Y, Ohta Y et al (2017) Anti-cancer stem cell activity of a hedgehog inhibitor GANT61 in estrogen receptor-positive breast cancer cells. Cancer Sci 108:918–930. https://doi.org/10.1111/cas.13205

Laplante M, Sabatini DM (2009) mTOR signaling at a glance. J Cell Sci 122:3589–3594. https://doi.org/10.1242/jcs.051011

Lathia JD, Mack SC, Mulkearns-Hubert EE et al (2015) Cancer stem cells in glioblastoma. Genes Dev 26:758. https://doi.org/10.1101/gad.261982.115.tumors

Lauth M, Toftgard R, Toftgård R (2007) Non-canonical activation of GLI transcription factors: implications for targeted anti-cancer therapy. Cell Cycle 6:2458–2463. https://doi.org/10.4161/cc.6.20.4808

Lee SY, Han HS, Lee KY et al (2007) Sonic hedgehog expression in gastric cancer and gastric adenoma. Oncol Rep 17:1051–1055

Livak KJ, Schmittgen TD (2001) Analysis of relative gene expression data using real-time quantitative PCR and the 2(-Delta Delta C(T)) method. Methods 25:402–408. https://doi.org/10.1006/meth.2001.1262

Louis DN, Perry A, Reifenberger G et al (2016) The 2016 World Health Organization classification of tumors of the central nervous system: a summary. Acta Neuropathol 131:803–820. https://doi.org/10.1007/s00401-016-1545-1

Maiuri MC, Zalckvar E, Kimchi A, Kroemer G (2007) Self-eating and self-killing: crosstalk between autophagy and apoptosis. Nat Rev Mol Cell Biol 8:741–752. https://doi.org/10.1038/nrm2239

Mao L, Xia YP, Zhou YN et al (2009) A critical role of Sonic Hedgehog signaling in maintaining the tumorigenicity of neuroblastoma cells. Cancer Sci 100:1848–1855. https://doi.org/10.1111/j.1349-7006.2009.01262.x

Matias D, Dubois LG, Pontes B et al (2018) GBM-derived Wnt3a induces M2-like phenotype in microglial cells through Wnt/β-catenin signaling. Mol Neurobiol 1–14: https://doi.org/10.1007/s12035-018-1150-5

Mazumdar T, DeVecchio J, Agyeman A et al (2011) Blocking Hedgehog survival signaling at the level of the GLI genes induces DNA damage and extensive cell death in human colon carcinoma cells. Cancer Res 71:5904–5914. https://doi.org/10.1158/0008-5472.CAN-10-4173

McKee CM, Xu D, Cao Y et al (2012) Protease nexin 1 inhibits hedgehog signaling in prostate adenocarcinoma. J Clin Investig 122:4025–4036. https://doi.org/10.1172/JCI59348

Mendell JT (2008) miRiad roles for the miR-17–92 cluster in development and disease. Cell 133:217–222

Mittal V (2018) Epithelial mesenchymal transition in tumor metastasis. Annu Rev Pathol Mech Dis 13:395–412

Nakada M, Kita D, Watanabe T et al (2011) Aberrant signaling pathways in glioma. Cancers (Basel) 3:3242–3278. https://doi.org/10.3390/cancers3033242

O'Donnell KA, Wentzel EA, Zeller KI et al (2005) c-Myc-regulated microRNAs modulate E2F1 expression. Nature. https://doi.org/10.1038/nature03677

Ostrom QT, Gittleman H, Truitt G et al (2018) CBTRUS statistical report: primary brain and other central nervous system tumors diagnosed in the United States in 2011–2015. Neuro Oncol 20:1–88

Pereira DL, dos Santos Ferreira AC, de Faria GP, Kwee JK (2015) Autophagy interplays with apoptosis and cell cycle regulation in the growth inhibiting effect of trisenox in HEP-2, a laryngeal squamous cancer. Pathol Oncol Res 21:103–111. https://doi.org/10.1007/s12253-014-9794-6

Ponnusamy MP, Batra SK (2008) Ovarian cancer: emerging concept on cancer stem cells. J Ovarian Res 1:4. https://doi.org/10.1186/1757-2215-1-4

Rossi M, Magnoni L, Miracco C et al (2011) β-catenin and Gli1 are prognostic markers in glioblastoma. Cancer Biol Ther 11:753–761

Roth W, Wild-Bode C, Platten M et al (2000) Secreted Frizzled-related proteins inhibit motility and promote growth of human malignant glioma cells. Oncogene 19:4210–4220. https://doi.org/10.1038/sj.onc.1203783

Schiapparelli P, Shahi MH, Enguita-German M et al (2011) Inhibition of the sonic hedgehog pathway by cyplopamine reduces the CD133+/CD15+ cell compartment and the in vitro tumorigenic capability of neuroblastoma cells. Cancer Lett 310:222–231. https://doi.org/10.1016/j.canlet.2011.07.005S0304-3835(11)00401-0

Shahi MH, Afzal M, Sinha S et al (2010) Regulation of sonic hedgehog-GLI1 downstream target genes PTCH1, Cyclin D2, Plakoglobin, PAX6 and NKX2.2 and their epigenetic status in medulloblastoma and astrocytoma. BMC Cancer 10:1–20. https://doi.org/10.1186/1471-2407-10-614

Shahi MH, Rey JA, Castresana JS (2012) The sonic hedgehog-GLI1 signaling pathway in brain tumor development. Expert Opin Ther Targets 16:1227–1238. https://doi.org/10.1517/14728222.2012.720975

Spohr TCL, Dezonne RS, Rehen SK, Gomes FCA (2011) Astrocytes treated by lysophosphatidic acid induce axonal outgrowth of cortical progenitors through extracellular matrix protein and epidermal growth factor signaling pathway. J Neurochem 119:113–123. https://doi.org/10.1111/j.1471-4159.2011.07421.x

Stockert JC, Horobin RW, Colombo LL, Blázquez-Castro A (2018) Tetrazolium salts and formazan products in cell biology: viability assessment, fluorescence imaging, and labeling perspectives. Acta Histochem 120:159–163

Sun Y, Guo W, Ren T et al (2014) Gli1 inhibition suppressed cell growth and cell cycle progression and induced apoptosis as well as autophagy depending on ERK1/2 activity in human chondrosarcoma cells. Cell Death Dis. https://doi.org/10.1038/cddis.2013.497

Taipale J, Chen JK, Cooper MK et al (2000) Effects of oncogenic mutations in Smoothened and Patched can be reversed by cyclopamine. Nature 406:1005–1009. https://doi.org/10.1038/35023008

Tang X, Deng L, Chen Q et al (2015) Inhibition of Hedgehog signaling pathway impedes cancer cell proliferation by promotion of autophagy. Eur J Cell Biol 94:223–233. https://doi.org/10.1016/j.ejcb.2015.03.003

Thomas HE, Zhang Y, Stefely JA et al (2018) Mitochondrial complex I activity is required for maximal autophagy. Cell Rep 24:2404–2417.e8. https://doi.org/10.1016/j.celrep.2018.07.101

Tong W, Qiu L, Qi M et al (2018) GANT-61 and GDC-0449 induce apoptosis of prostate cancer stem cells through a GLI-dependent mechanism. J Cell Biochem 119:3641–3652. https://doi.org/10.1002/jcb.26572

Uziel T, Karginov FV, Xie S et al (2009a) The miR-17~92 cluster collaborates with the Sonic Hedgehog pathway in medulloblastoma. Proc Natl Acad Sci USA 106:2812–2817

Uziel T, Karginov FV, Xie S et al (2009b) The miR-17~92 cluster collaborates with the Sonic Hedgehog pathway in medulloblastoma. Proc Natl Acad Sci USA 106:2812–2817. https://doi.org/10.1073/pnas.08095791060809579106

Villavicencio EH, Walterhouse DO, Iannaccone PM (2000) The Sonic hedgehog-Patched-Gli pathway in human development and disease. Am J Hum Genet. https://doi.org/10.1016/S0002-9297(07)62934-6

Von Hoff DD, LoRusso PM, Rudin CM et al (2009) Inhibition of the hedgehog pathway in advanced basal-cell carcinoma. N Engl J Med 361:1164–1172. https://doi.org/10.1056/NEJMoa0905360NEJMoa0905360 [pii]

Wang J, Gu S, Huang J et al (2014) Inhibition of autophagy potentiates the efficacy of Gli inhibitor GANT-61 in MYCN-amplified neuroblastoma cells. BMC Cancer. https://doi.org/10.1186/1471-2407-14-768

Wang J, Huang S, Tian R et al (2018) The protective autophagy activated by GANT-61 in MYCN amplified neuroblastoma cells is mediated by PERK. Oncotarget 9:14413–14427. https://doi.org/10.18632/oncotarget.24214

Wang S, Lu S, Geng S et al (2013a) Expression and clinical significance of microRNA-326 in human glioma miR-326 expression in glioma. Med Oncol. https://doi.org/10.1007/s12032-012-0373-y

Wang Y, Han C, Lu L et al (2013b) Hedgehog signaling pathway regulates autophagy in human hepatocellular carcinoma cells. Hepatology 58:995–1010. https://doi.org/10.1002/hep.26394

Xu JH, Yang HP, Zhou XD et al (2015) Autophagy accompanied with bisdemethoxycurcumin-induced apoptosis in non-small cell lung cancer cells. Biomed Environ Sci 28:105–115. https://doi.org/10.3967/bes2015.013

Yin S, Du W, Wang F et al (2016) MicroRNA-326 sensitizes human glioblastoma cells to curcumin via the SHH/GLI1 signaling pathway. Cancer Biol Ther. https://doi.org/10.1080/15384047.2016.1250981

Zheng X, Zeng W, Gai X et al (2013) Role of the Hedgehog pathway in hepatocellular carcinoma (Review). Oncol Rep 30:2020–2026

Zhu H, Carpenter RL, Han W, Lo HW (2014) The GLI1 splice variant TGLI1 promotes glioblastoma angiogenesis and growth. Cancer Lett 343:51–61. https://doi.org/10.1016/j.canlet.2013.09.014

Zindy F, Kawauchi D, Lee Y et al (2014) Role of the miR-17 92 cluster family in cerebellar and medulloblastoma development. Biol Open 3:597–605. https://doi.org/10.1242/bio.20146734